


# Deletion of *PHO13*, Encoding Haloacid Dehalogenase Type IIA Phosphatase, Results in Upregulation of the Pentose Phosphate Pathway in *Saccharomyces cerevisiae*

Soo Rin Kim,<sup>a</sup> Haiqing Xu,<sup>b</sup> Anastashia Lesmana,<sup>c</sup> Uros Kuzmanovic,<sup>c</sup> Matthew Au,<sup>d</sup> Clarissa Florencia,<sup>b</sup> Eun Joong Oh,<sup>b</sup> Guochang Zhang,<sup>b</sup>  Kyoung Heon Kim,<sup>e</sup> Yong-Su Jin<sup>b,c</sup>

School of Food Science and Biotechnology, Kyungpook National University, Daegu, Republic of Korea<sup>a</sup>; Department of Food Science and Human Nutrition, University of Illinois at Urbana-Champaign, Urbana, Illinois, USA<sup>b</sup>; Institute for Genomic Biology, University of Illinois at Urbana-Champaign, Urbana, Illinois, USA<sup>c</sup>; Department of Chemical Engineering, University of Illinois at Urbana-Champaign, Urbana, Illinois, USA<sup>d</sup>; Department of Biotechnology, Korea University Graduate School, Seoul, Republic of Korea<sup>e</sup>

The haloacid dehalogenase (HAD) superfamily is one of the largest enzyme families, consisting mainly of phosphatases. Although intracellular phosphate plays important roles in many cellular activities, the biological functions of HAD enzymes are largely unknown. Pho13 is 1 of 16 putative HAD enzymes in *Saccharomyces cerevisiae*. Pho13 has not been studied extensively, but previous studies have identified *PHO13* to be a deletion target for the generation of industrially attractive phenotypes, namely, efficient xylose fermentation and high tolerance to fermentation inhibitors. In order to understand the molecular mechanisms underlying the improved xylose-fermenting phenotype produced by deletion of *PHO13* (*pho13Δ*), we investigated the response of *S. cerevisiae* to *pho13Δ* at the transcriptomic level when cells were grown on glucose or xylose. Transcriptome sequencing analysis revealed that *pho13Δ* resulted in upregulation of the pentose phosphate (PP) pathway and NADPH-producing enzymes when cells were grown on glucose or xylose. We also found that the transcriptional changes induced by *pho13Δ* required the transcription factor Stb5, which is activated specifically under NADPH-limiting conditions. Thus, *pho13Δ* resulted in the upregulation of the PP pathway and NADPH-producing enzymes as a part of an oxidative stress response mediated by activation of Stb5. Because the PP pathway is the primary pathway for xylose, its upregulation by *pho13Δ* might explain the improved xylose metabolism. These findings will be useful for understanding the biological function of *S. cerevisiae* Pho13 and the HAD superfamily enzymes and for developing *S. cerevisiae* strains with industrially attractive phenotypes.

Phosphate, one of the most abundant intracellular molecules, is carried in ATP and transferred to many other metabolites and proteins (1). Phosphate starvation in medium results in cell cycle arrest at the G<sub>1</sub> stage (2). Moreover, the intracellular inorganic phosphate pool mediates the proper initiation and homeostasis of metabolic flux in the glycolytic pathway (3). In signal transduction pathways, protein phosphorylation plays a key role by regulating protein localization, protein interactions, and enzyme activity (4).

The haloacid dehalogenase (HAD) superfamily is one of the largest enzyme families, consisting of ~80,000 sequences that encode proteins whose functions are largely unknown (5). The family name originated from the first enzyme that was structurally characterized (6), but 70% of the family members are phosphatases (<http://sflld.rbvi.ucsf.edu/django/superfamily/>). The active site of HAD enzymes consists of highly conserved core domains and a versatile cap domain (7, 8). The presence and location of the cap domain allow diverse substrate specificities, which form the basis for the classification of the enzymes into several subfamilies (7).

*Saccharomyces cerevisiae* Pho13 is structurally classified as a member of HAD subfamily IIA (9), which contains ~3,000 sequences, including eukaryotic 2-phosphoglycolate phosphatase (PGP or PGLP) and pyridoxal phosphatase. Although two bacterial enzymes, AraL from *Bacillus subtilis* (a Gram-positive bacterium) and NagD from *Escherichia coli* (a Gram-negative bacterium), are classified into this subfamily as well, their biochemical properties differ from those of eukaryotic enzymes (9, 10). Moreover, the physiological importance of this group of enzymes is not yet understood.

Although little is known about the biochemical and physiological functions of *S. cerevisiae* Pho13, deletion of the *PHO13* gene (*pho13Δ*) results in significant and industrially relevant phenotypic changes in engineered strains capable of fermenting xylose (11–16). Introduction of a heterologous metabolic pathway consisting of either xylose reductase/xyloitol dehydrogenase/xyloketonase [X(R/X)D(H/X)K] or xylose isomerase/xyloketonase [X(I/X)K] allows *S. cerevisiae* to metabolize xylose (17). However, the rates of xylose metabolism in the engineered strains are lower than those of glucose metabolism. In one study, random transposon mutagenesis of an *S. cerevisiae* strain overexpressing X(R/X)D(H/X)K generated a mutant strain with an insertional mutation in

Received 22 October 2014 Accepted 15 December 2014

Accepted manuscript posted online 19 December 2014

Citation Kim SR, Xu H, Lesmana A, Kuzmanovic U, Au M, Florencia C, Oh EJ, Zhang G, Kim KH, Jin Y-S. 2015. Deletion of *PHO13*, encoding haloacid dehalogenase type IIA phosphatase, results in upregulation of the pentose phosphate pathway in *Saccharomyces cerevisiae*. *Appl Environ Microbiol* 81:1601–1609. doi:10.1128/AEM.03474-14.

Editor: A. A. Brakhage

Address correspondence to Soo Rin Kim, soorinkim@knu.ac.kr, or Yong-Su Jin, ysjin@illinois.edu.

Supplemental material for this article may be found at <http://dx.doi.org/10.1128/AEM.03474-14>.

Copyright © 2015, American Society for Microbiology. All Rights Reserved. doi:10.1128/AEM.03474-14

*PHO13* that grew much better on xylose (11). In another independent study, adaptive evolution of an *S. cerevisiae* strain overexpressing X(R/X)D(H/X)K on xylose led to a spontaneous single nucleotide polymorphism (SNP) in *PHO13*, which increased xylose consumption 5-fold (12). In both cases, the loss of Pho13 function (*pho13Δ*) was shown to be responsible for the improvement in xylose metabolism (12, 14). Moreover, *pho13Δ* in *S. cerevisiae* strains overexpressing X(R/X)D(H/X)K improved tolerance to common fermentation inhibitors (weak acids and sugar degradation products) (13, 15). In addition to its effects in strains overexpressing X(R/X)D(H/X)K, *pho13Δ* in a strain overexpressing X(I/X)K improved the growth rate on xylose 8-fold (16). Thus, different research groups have confirmed the positive effect of *pho13Δ* on xylose metabolism in both xylose pathways and in various strain backgrounds. As such, there is a need to determine the biological function of the Pho13 enzyme and the mechanism underlying the effect of *pho13Δ* on xylose metabolism.

This study focused on the Pho13 enzyme. In transcriptome sequencing (RNA-seq) analysis, we found that *pho13Δ* induced transcriptional changes when cells were grown on xylose or glucose. We propose that *pho13Δ* triggers transcriptional reprogramming, which directly improves xylose metabolism in engineered *S. cerevisiae* strains capable of fermenting xylose.

## MATERIALS AND METHODS

**Strain construction.** To construct the *pho13Δ* and *stb5Δ* mutants, PCR-based gene deletion (18) was performed using the plasmids and primers listed in Tables 1 and 2. Specifically, using a pUG6 plasmid as the template, the *kanMX* marker gene with *PHO13*-specific overhanging sequences (the nucleotide sequence in lowercase letters in Table 2) was amplified using primers SOO615 and SOO428. The PCR product was purified and transformed into yeast strains using the lithium acetate/single-stranded carrier DNA–polyethylene glycol method (19). The *pho13Δ::kanMX* deletion mutant was selected on YPD (10 g/liter yeast extract, 20 g/liter peptone, 20 g/liter glucose) agar medium containing 300 μg/ml G418. To construct the *stb5Δ::hghMX* mutant, a pUG75 plasmid, the SOO411 and SOO412 primers, and YPD agar medium containing 300 μg/ml hygromycin B were used instead. Several colonies were confirmed through colony PCR using primers that amplified each end of the integration site: SOO575/SOO148 and SOO576/SOO149 for *pho13Δ::kanMX* and SOO431/SOO148 and SOO455/SOO149 for *stb5Δ::hghMX*.

**Strain construction using CRISPR-Cas.** The following method was modified from the first paper describing *S. cerevisiae* genome engineering with a clustered regularly interspaced short palindromic repeat (CRISPR)-Cas system (20), as follows. (i) p41N-Cas9 was constructed by transferring the Cas9 cassette from the p414-TEF1p-Cas9-CYC1t plasmid (Addgene) to p41N, a single-copy plasmid containing a *natMX* marker.

(ii) Guide RNA (gRNA) with 20 bp of a *GND1.1*-specific sequence was designed as described in Table 3. The *GND1.1*-specific sequence was the only modification to the gRNA described previously (20). It was chosen from the sequence immediately 5' of the NGG protospacer-associated motif (PAM) sequence, which was located in the *Stb5*-binding sequence (CGGTGTTA, where the PAM sequence is underlined). The gRNA was synthesized by IDT (Coralville, IA, USA) as gBlocks gene fragments with 5' phosphorylated ends. The gBlocks gene fragments were then ligated with a p42H vector that had been linearized and dephosphorylated by treatment with EcoRV and rSAP. The resulting plasmid, p42H-*GND1.1*, was treated with BamHI and SalI to confirm the presence of the insert.

(iii) Donor DNA was PCR amplified using the primers SOO567/SOO568, which generated double-stranded DNA of 100 bp that covered the *GND1.1*-specific sequence area and contained a mutation in the *Stb5*-binding sequence (CIGTGTTA, where the mutation is underlined). Because the mutation site overlapped the PAM sequence, there was no need

TABLE 1 Plasmids and strains used in this study

Plasmid or strain	Description	Reference or source
<b>Plasmids</b>		
pUG6	A template plasmid containing a <i>kanMX</i> marker for PCR-based gene knockout	30
pUG75	A template plasmid containing an <i>hphMX</i> marker for PCR-based gene knockout	18
p41N-Cas9	A single-copy plasmid containing Cas9 and a <i>natMX</i> marker	This study
p42H- <i>GND1.1</i>	A multicopy plasmid containing a gRNA and an <i>hphMX</i> marker	This study
p41K- <i>TEF1<sub>p</sub></i> - <i>STB5</i>	A single-copy plasmid containing <i>STB5</i> under the control of the <i>TEF1</i> promoter and a <i>kanMX</i> marker	This study
<b>Strains</b>		
BY4742	A laboratory wild-type strain of <i>S. cerevisiae</i>	31
BY4742 <i>pho13Δ</i>	BY4742 <i>pho13::kanMX</i>	32
D452-2	A laboratory wild-type strain of <i>S. cerevisiae</i>	33
D452-2 <i>pho13Δ</i>	D452-2 <i>pho13::kanMX</i>	This study
SR7	D452-2 with a xylose pathway ( <i>S. stipitis</i> <i>XYL1</i> , <i>XYL2</i> , and <i>XYL3</i> )	12
SR7 <i>pho13Δ</i>	SR7 <i>pho13::kanMX</i>	12
SR7 <i>stb5Δ</i>	SR7 <i>stb5::hphMX</i>	This study
SR7 <i>pho13Δ stb5Δ</i>	SR7 <i>pho13::kanMX stb5::hphMX</i>	This study
SR7 <i>pho13Δ</i> Cas9	SR7 <i>pho13Δ</i> pRS41N-Cas9	This study
SR7 <i>pho13Δ GND1.1</i>	SR7 <i>pho13Δ</i> with a mutation in the upstream <i>GND1</i>	This study
SR7 <i>TEF1<sub>p</sub></i> - <i>STB5</i>	SR7 p41K- <i>TEF1<sub>p</sub></i> - <i>STB5</i>	This study

to introduce an additional mutation in the PAM sequence to prevent gRNA binding.

(iv) The target strain (SR7 *pho13Δ*) was first transformed with p41N-Cas9 and plated on a YPD agar plate containing 120 μg/ml nourseothricin (clonNAT). The resulting strain was transformed with the p42H-*GND1.1* plasmid and donor DNA and plated on a YPD agar plate containing 120 μg/ml nourseothricin and 300 μg/ml hygromycin B. The colonies were restreaked on the same type of agar plates, and the mutation was confirmed by sequencing 1 kb upstream of *GND1*.

**Culture conditions.** All strains were aerobically precultured in 5 ml of YPD at 30°C for 24 h. For the growth profile and RNA extraction, precultured cells were inoculated into 50 ml of YP (yeast extract-peptone) medium containing either 40 g/liter glucose or 40 g/liter xylose at an initial cell density of  $2 \times 10^6$  cells. For sugar fermentation, precultured cells were inoculated into 50 ml of YP medium containing both 40 g/liter glucose and 40 g/liter xylose at an initial cell density of  $2 \times 10^7$  cells. The culture was incubated in a 250-ml Erlenmeyer flask at 30°C and 100 rpm. RNA was extracted when the absorbance at 600 nm ( $A_{600}$ ) reached 1, as shown in Fig. 1. For testing of cell growth on xylose, a Bioscreen C plate reader system was used (Growth Curves USA, Piscataway, NJ) as previously described (12).

**RNA extraction.** For RNA-seq and reverse transcription (RT)-quantitative PCR (qPCR), RNA was extracted from the fresh cultures described above. First,  $1 \times 10^7$  cells (equivalent to an  $A_{600}$  of 0.5) were harvested and resuspended in a buffer containing 1 M sorbitol, 0.1 M EDTA, 0.1% 2-mercaptoethanol, and 50 U Zymolyase (pH 7.4). The solution was incubated at 30°C and 100 rpm for 30 min to generate spheroplasts. RNA

TABLE 2 Primers used in this study

Name	Sequence <sup>a</sup>	Description <sup>b</sup>
SOO615	5'-tatcaagctcgagcacaatcacaaaaagccttatagcttgcctgacaaaagaatatacaactcgggaaaCAGCTGAAGCTTCGTACGC	<i>pho13::loxP</i> -F
SOO428	5'-aaaacaacaacacgaatattttcttttcaaaaagtaattctaccctagattttgcatctctGCATAGGCCACTAGTGGATCTG	<i>pho13::loxP</i> -R
SOO411	5'-cgtaacaagaggataatcatcagcgtacagggtcaaaaaattaatacaaaaggtgtaaaagaaggacatgCAGCTGAAGCTTCGTACGC	<i>stb5::loxP</i> -F
SOO412	5'-ttaaaggcagcaacaagcgtcctgtagtagtagcagcatgacaaaactcggggaacatatgtcaGCATAGGCCACTAGTGGATCTG	<i>stb5::loxP</i> -R
SOO575	5'-GCCGGATCCACTGTGATACTAACGGGCAACTAC	<i>PHO13_883</i> -up-F
SOO576	5'-GCCGTCGACGAATTGGTCAACACTCTGAGCG	<i>PHO13_384</i> -down-R
SOO431	5'-GCGCTTAGCACTGTTGAATC	<i>STB5_527</i> -up-F
SOO455	5'-AAGTTCCGCCTCTTGGAGAC	<i>STB5_434</i> -down-R
SOO148	5'-GGATGTATGGGCTAAATG	B-M (paired with up)
SOO149	5'-CCTCGACATCATCTGCC	C-M (paired with down)
SOO613	5'-GCCTTCTACGTTTCCATCCA	RT-qPCR_ <i>ACT1</i> -F
SOO614	5'-GGCCAAATCGATTCTCAAAA	RT-qPCR_ <i>ACT1</i> -R
SOO355	5'-TGCTCGTTATGCGTCTTATCC	RT-qPCR_ <i>ZWF1</i> -F
SOO356	5'-CTGCACCTGTGGCAATTATTC	RT-qPCR_ <i>ZWF1</i> -R
SOO429	5'-GCGGACGAATCACTATCTTCTC	RT-qPCR_ <i>SOL3</i> -F
SOO430	5'-GCTCTTGAAGGCACCATAA	RT-qPCR_ <i>SOL3</i> -R
SOO417	5'-CTGCTACTTATGGCTGGAAACT	RT-qPCR_ <i>GND1</i> -F
SOO418	5'-GGTCTTCTCTGTAGGCCTTTG	RT-qPCR_ <i>GND1</i> -R
SOO365	5'-CCTCAAGACTCCACAATAACC	RT-qPCR_ <i>TAL1</i> -F
SOO366	5'-ACCATGCTTCTACCGTATTCC	RT-qPCR_ <i>TAL1</i> -R
SOO567	5'-TTGTACCTATTGTGGCTGTGGTGTACATTACGGTGCCTC <u>IGT</u> GTTACGCGGTGCTTCG	<i>GND1.1</i> _Donor-F
SOO568	5'-CCACCAAGGCCAAAGCGCAAGGCCGCTGGACCACCAGGACGAAGCACC CGTAAACAC <u>AG</u>	<i>GND1.1</i> _Donor-R

<sup>a</sup> Lowercase nucleotides indicate *PHO13*-specific overhanging sequences; the underlined nucleotide in SOO568 represents a SNP.

<sup>b</sup> F, forward; R, reverse.

was immediately extracted using a Qiagen RNeasy minikit. The RNA yield was 10 to 40  $\mu$ g.

**RNA-seq.** The concentration and quality of the RNA samples were evaluated on a Bioanalyzer RNA chip. Samples with high-quality total RNA were used to construct a bar-coded library with poly(A)<sup>+</sup> RNA. Sequencing was performed on an Illumina HiSeq 2000 system at the W. M. Keck Center for Comparative and Functional Genomics at the University of Illinois at Urbana-Champaign. The detailed procedure for Illumina sequencing has been described previously (12). The sequencing results were analyzed using the CLC Genomic Workbench (version 6.5) program as follows. First,  $\sim$ 100-bp sequencing reads (fastq files) were trimmed and mapped to the *S. cerevisiae* S288C reference genome sequence modified with a xylose pathway. All mapped reads at exons were counted, and the numbers were converted to the total number of exon reads per kilobase of exon length per million mapped reads (RPKM). The numbers of RPKM from three biological replicates of the *pho13* $\Delta$  strain were compared to those of the wild-type strain, and *t* tests were applied. Finally, genes with significantly different expression levels ( $>2$ -fold,  $P < 0.05$ ) were identified (see Data Set S1 in the supplemental material).

**RT-qPCR of pentose phosphate (PP) pathway genes.** For quantitative PCR with RNA samples (RT-qPCR), cDNA was generated from 1  $\mu$ g

of RNA using iScript reverse transcription supermix (Bio-Rad, Hercules, CA, USA). Then, cDNA solution (1  $\mu$ l) was used directly for qPCR with prepared primer solutions and SYBR green I master mix (Roche Applied Science, Indianapolis, IN, USA). qPCRs were performed in a 96-well plate on a LightCycler 480 apparatus (Roche). All primers (Table 2) were designed using the IDT PrimerQuest program.

The qPCR results were calculated by the comparative threshold cycle ( $C_T$ ) method (the  $\Delta\Delta C_T$  method) (21). Specifically, the transcript abundance (the change in the  $C_T$  [ $\Delta C_T$ ]  $\pm s$  [where  $s$  is the standard deviation of the  $\Delta C_T$  value]) of a target gene (*ZWF1*, *SOL3*, *GND1*, and *TAL1*) relative to that of a reference gene (*ACT1*) was calculated from three biological replicates. The difference in the  $\Delta C_T$  value ( $\Delta\Delta C_T \pm s$  [where  $s$  is the standard deviation of the  $\Delta C_T$  value of a *pho13* $\Delta$  mutant]) for a *pho13* $\Delta$  mutant compared to that for a wild-type strain was then converted into a fold change [ $2^{(-\Delta\Delta C_T)}$ ] with an error range [ $2^{(-\Delta\Delta C_T + s)} - 2^{(-\Delta\Delta C_T - s)}$ ].

## RESULTS

***pho13* $\Delta$  enhances xylose metabolism but does not affect glucose metabolism.** To characterize the phenotypic changes induced by

TABLE 3 gRNA (gBlocks) sequences (388 bp)

Parts	Sequence	Length (bp)
<i>SNR52</i> promoter	TCTTTGAAAAGATAATGTATGATTATGCTTTCACTCATATTTATACAGAACTTGATGTTTTCTTTTCGAGTATA TACAAGGTGATTACATGTACGTTTGAAGTACAACCTAGATTTTGTAGTGCCCTCTTGGGCTAGCGGTAA AGGTGCGCATTTTTTTCACACCCTACAATGTTCTGTTCAAAAAGATTTTGGTCAAACGCTGTAGAAGTAAAA GTTGGTGCATGTTTCGGCGTTCGAAACTTCTCCGCAGTGAAAGATAAATGATC	269
<i>GND1.1</i> gRNA (target specific)	GGTGTACATTACGGTGCCT	20
Structural crRNA	GTTTTAGAGCTAGAAATAGCAAGTTAAATAAGGCTAGTCCGTTATCAACTTGAAAAAGTGGCACCGAGTCGG TGGTGC	79
<i>SUP4</i> terminator	TTTTTTGTTTTTATGCT	20

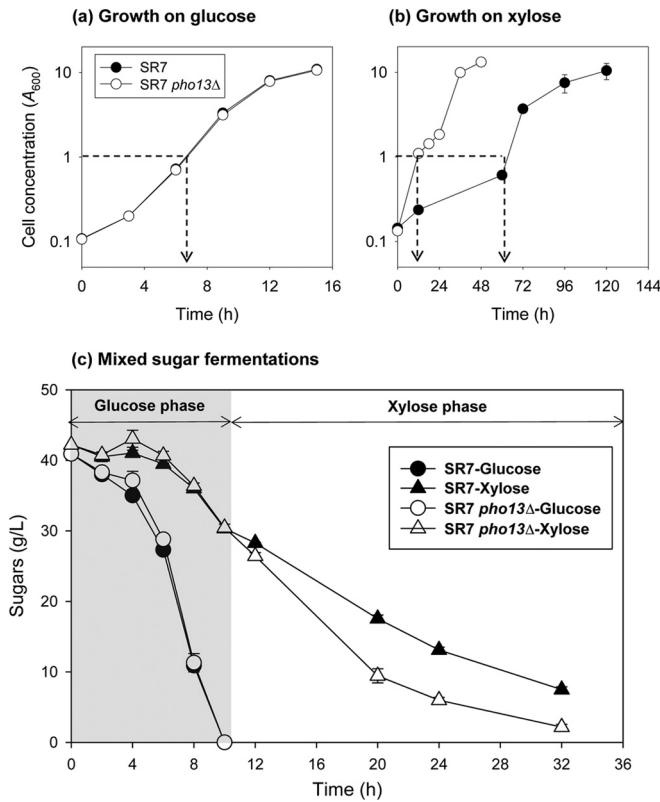


**FIG 1** *pho13Δ* significantly improves the xylose metabolism of the mutant, while there is no visible effect when the cells are metabolizing glucose (overlapping symbols). Cell growth was measured during growth on a single carbon source, glucose (a) or xylose (b). (c) Sugar consumption was measured during growth on a mixture of glucose and xylose, and the results from the two strains were combined. When cells reached the mid-exponential phase (arrows in panels a and b), samples were collected for RNA extraction.

*pho13Δ*, we compared wild-type and *pho13Δ* mutant strains of xylose-fermenting *S. cerevisiae* SR7 grown under glucose (Fig. 1a), xylose (Fig. 1b), and the mixed sugar (Fig. 1c) conditions. The SR7 strain, created from the wild-type *S. cerevisiae* D452-2 strain, contains a heterologous xylose metabolic pathway consisting of the *Scheffersomyces stipitis* *XYL1*, *XYL2*, and *XYL3* genes (12). When

the strains were grown on glucose, no phenotypic differences were observed (Fig. 1a). However, when the strains were grown on xylose, the SR7 *pho13Δ* strain grew significantly faster than the SR7 strain (Fig. 1b). Specifically, the SR7 *pho13Δ* strain grew from a cell density ( $A_{600}$ ) of 0.1 to one of 1 in 12 h, while the SR7 strain took four times longer. When fermenting a mixture of glucose and xylose (Fig. 1c), the growth differences between the SR7 and SR7 *pho13Δ* strains were not as obvious as the growth differences on xylose only. However, during a xylose-consuming phase followed by a glucose-consuming phase, the xylose consumption rate of the SR7 *pho13Δ* strain was faster than that of the SR7 strain, which confirmed that the metabolic benefits induced by *pho13Δ* were specific to xylose metabolism and consistent for the single sugar and the mixed sugar fermentations (Fig. 1c).

***pho13Δ* induces the PP pathway and NADPH gene expression regardless of the type of sugar substrate.** To elucidate the mechanisms underlying the phenotypic changes induced by *pho13Δ*, the global transcript profiles of SR7 and SR7 *pho13Δ* grown in glucose or xylose were analyzed. Three biological replicates of RNA samples were subjected to RNA-seq. The genes differentially expressed (DE; >2-fold) in the *pho13Δ* strain compared to their expression in the wild-type strain when the strains were grown in the same sugar were identified with a *P* value of <0.05 (see Data Set S1 in the supplemental material). Although the deletion phenotype was observed only in cells grown on xylose (Fig. 1), transcriptional changes induced by *pho13Δ* were observed with both glucose and xylose: 12 DE genes were detected for growth on glucose, and 277 DE genes were detected for growth on xylose (Fig. 2). When those DE genes were presented on the basis of the direction of changes, we found that 9 genes were upregulated under both conditions (Table 4). Most genes were directly or indirectly involved in NADPH regeneration: PP pathway genes (*GND1*, *SOL3*, and *TAL1*), NADPH-specific oxidoreductase genes (*GCY1* and *GOR1*), and NADH kinase genes (*YEF1*). These results suggest that the loss of Pho13 induces the transcriptional upregulation of genes involved in the PP pathway and redox balance.

***pho13Δ* upregulates fermentative pathways under xylose conditions.** In terms of the numbers of genes affected and the degree of changes, *pho13Δ* had greater effects during xylose metabolism than during glucose metabolism. We reasoned that the

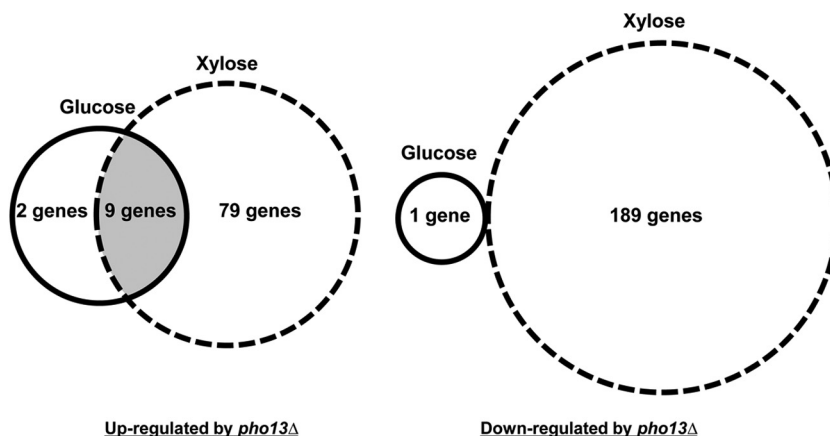


**FIG 2** Number of genes upregulated and downregulated (>2-fold, *P* < 0.05) by *pho13Δ* during exponential growth on glucose and xylose.



**TABLE 4** Nine genes upregulated<sup>a</sup> by the *pho13Δ* strain on both glucose and xylose

Gene name	Fold change in expression <sup>b</sup>		Function	Pathway
	Glucose	Xylose		
<i>SOL3</i>	6.2	8.8	6-Phosphogluconolactonase	PP pathway
<i>GND1</i>	6.8	15.0	6-Phosphogluconate dehydrogenase	PP pathway
<i>TAL1</i>	3.5	4.2	Transaldolase	PP pathway
<i>GCY1</i>	5.1	7.8	Glycerol dehydrogenase	NADPH regeneration
<i>GOR1</i>	4.1	5.3	Glyoxylate reductase	NADPH regeneration
<i>YEF1</i>	2.6	13.8	ATP-NADH kinase	NADPH regeneration
<i>YDR248C</i>	4.3	4.9	Putative gluconokinase	
<i>YHR182C-A</i>	6.0	16.6	Transposable element gene	
<i>YLR152C</i>	4.4	6.0	Uncharacterized	

<sup>a</sup> Upregulated >2-fold ( $P < 0.05$ ). None of the genes was downregulated.

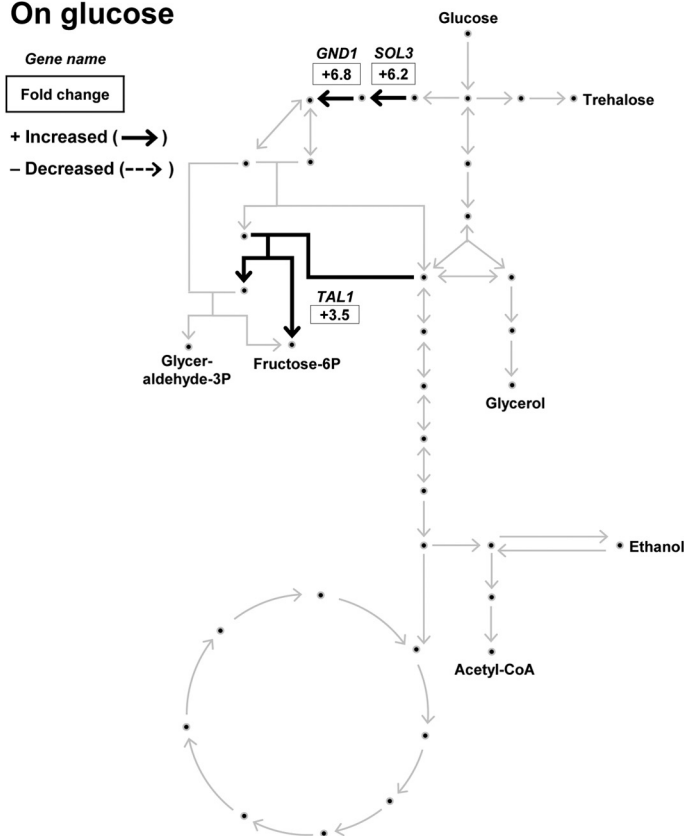
<sup>b</sup> Relative number of reads per kilobase of exon length per million reads (RPKM) of the *pho13Δ* mutant compared to that of the wild-type strain.

*pho13Δ*-induced changes in the transcriptional profile in cells grown on xylose might be related to the phenotypic improvement in xylose metabolism (Fig. 1). To confirm this hypothesis, we investigated the transcriptional changes of genes in central meta-

bolic pathways (the PP pathway, glycolysis, and the tricarboxylic acid [TCA] cycle) (Fig. 3). When cells were grown on xylose, most genes involved in the PP pathway and fermentative metabolism (glycolysis and ethanol production) were upregulated by *pho13Δ* (black-line arrows in Fig. 3). On the other hand, some genes involved in respiratory metabolism (TCA cycle and ethanol utilization) were downregulated (dotted-line arrows in Fig. 3). The *RK11* gene, coding for ribose-5-phosphate (ribose-5P) isomerase, was the only gene from the PP pathway that was downregulated by *pho13Δ*. Because ribose-5P is a precursor for the histidine, purine, and pyrimidine biosynthetic pathways, the *RK11* gene was considered a component of anabolic metabolism. In summary, the *pho13Δ* mutant induced transcriptomic changes that were favorable for xylose fermentation.

**The *pho13Δ*-induced upregulation of the PP pathway genes is not specific to the strain background.** To confirm the RNA-seq results, RT-qPCR was performed to assess *SOL3*, *GND1*, and *TAL1* gene expression using RNA samples from strains SR7 and SR7 *pho13Δ* grown on glucose. As a negative control, *ZWF1* (encoding glucose-6-phosphate dehydrogenase) was also tested because its transcript abundance was not affected by *pho13Δ* when cells were grown on glucose. The transcript abundance of the three genes was 4- to 8-fold higher in the SR7 *pho13Δ* strain than in the SR7 strain (Fig. 4), in agreement with the RNA-seq results. To determine if the transcriptional changes induced by *pho13Δ* were associated with the heterologous xylose pathway in SR7 or were

### On glucose



### On xylose

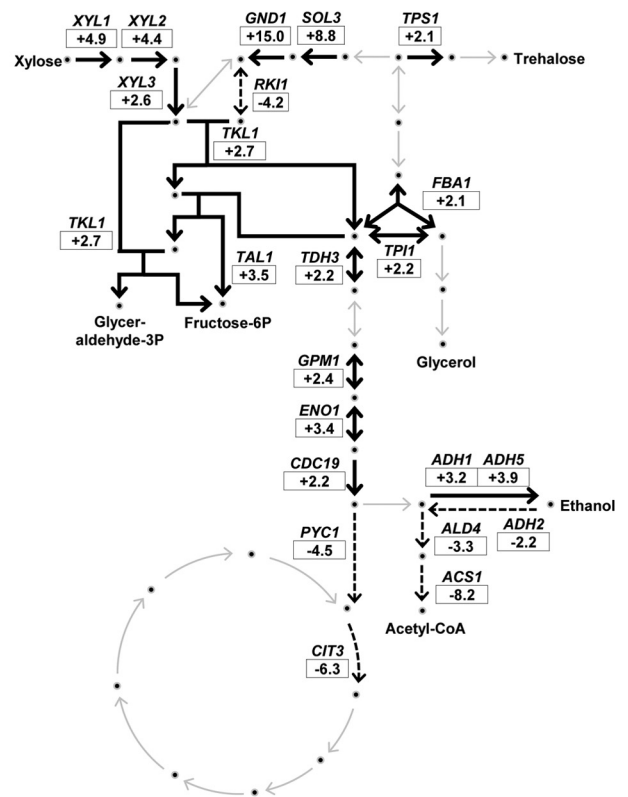


**FIG 3** Transcriptomic changes in central metabolic pathways induced by *pho13Δ* during growth on different carbon sources. The fold change in expression in the *pho13Δ* mutant relative to that in the wild-type strain is presented. Glyceraldehyde-3P, glyceraldehyde-3-phosphate; Fructose-6P, fructose-6-phosphate; Acetyl-CoA, acetyl coenzyme A.

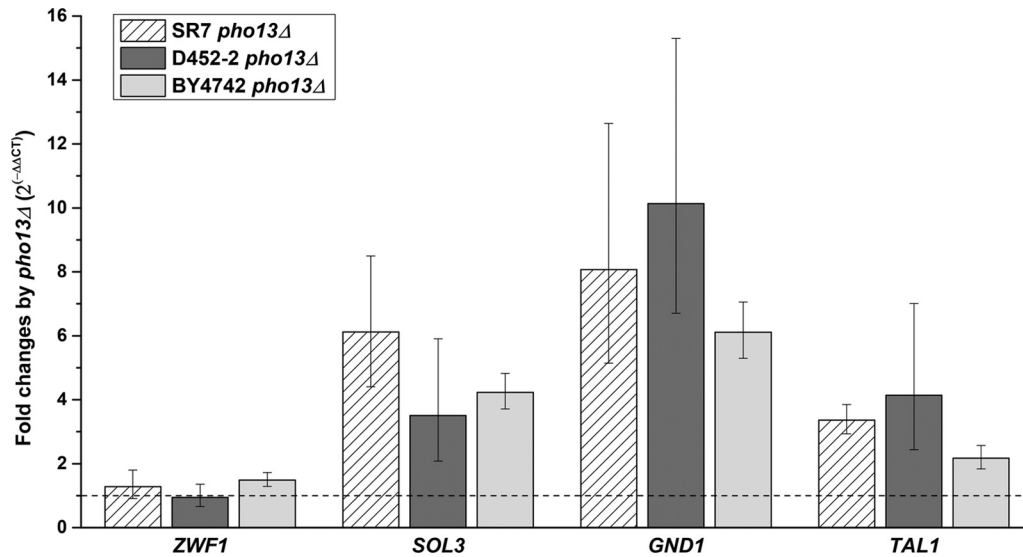


FIG 4 RT-qPCR confirmation of transcriptional changes induced by *pho13Δ* in three different strain backgrounds. The fold change in expression in the *pho13Δ* mutant relative to that in the corresponding wild-type strain is presented. Three genes (*SOL3*, *GND1*, and *TAL1*) upregulated by *pho13Δ* were tested along with one gene that was not affected (*ZWF1*); all genes are in the pentose phosphate pathway. A fold change of 1 (dashed line) indicates no change in the level of transcription.

dependent on the strain background (*S. cerevisiae* D452-2), RT-qPCR for the same gene set was performed to assess transcripts in the D452-2 *pho13Δ* and BY4742 *pho13Δ* strains, with the respective wild-type strains being used as controls. In both *pho13Δ* strains, the *SOL3*, *GND1*, and *TAL1* genes were upregulated, while *ZWF1* expression remained the same. These results suggest that the transcriptional upregulation induced by the loss of Pho13 did not depend either on the xylose pathway or on the strain background.

**Transcription factor Stb5 is upregulated by *pho13Δ*.** The RNA-seq and RT-qPCR results indicated that *pho13Δ* resulted in global transcriptional changes. Because Pho13 does not have a DNA binding domain, we hypothesized that at least one transcription factor was involved in the *pho13Δ*-induced transcriptional changes. However, we did not find any transcription factors that were differentially expressed (>2-fold,  $P < 0.05$ ) by *pho13Δ* in our RNA-seq results (see Data Set S1 in the supplemental material). To detect minor changes in the expression of transcription factors, the RNA-seq data were reprocessed using a  $P$  value of

<0.05. With this criterion, 30 transcription factors were differentially expressed because of *pho13Δ* in cells grown on glucose or xylose (Fig. 5). Among the six transcription factors that were differentially expressed in the *pho13Δ* strain on glucose, *STB5* was the only gene that was regulated in the same direction (upregulation) under both conditions (1.3-fold increase on glucose and 1.5-fold increase on xylose). *YAP5* was upregulated during growth on glucose but downregulated during growth on xylose. *STB5* is a zinc finger protein that upregulates PP pathway and NADPH-producing genes under oxidative stress and NADPH limitation (22, 23). The results suggest that Stb5 mediates the transcriptional changes induced by *pho13Δ*.

**Stb5 is required for the transcriptional changes induced by *pho13Δ*.** To determine if Stb5 plays a role in the transcriptional changes induced by *pho13Δ*, the transcript abundance of the gene that was the most strongly upregulated by *pho13Δ*, *GND1*, was compared in strains lacking *PHO13* or *STB5* (Fig. 6). The relative expression of *GND1* was significantly higher in the *pho13Δ* mutant than in the wild-type strain, as found earlier. However, in the

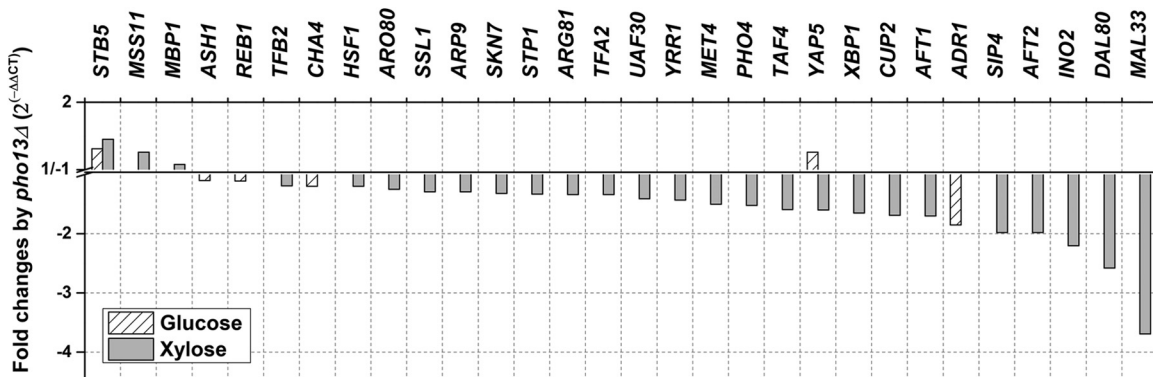
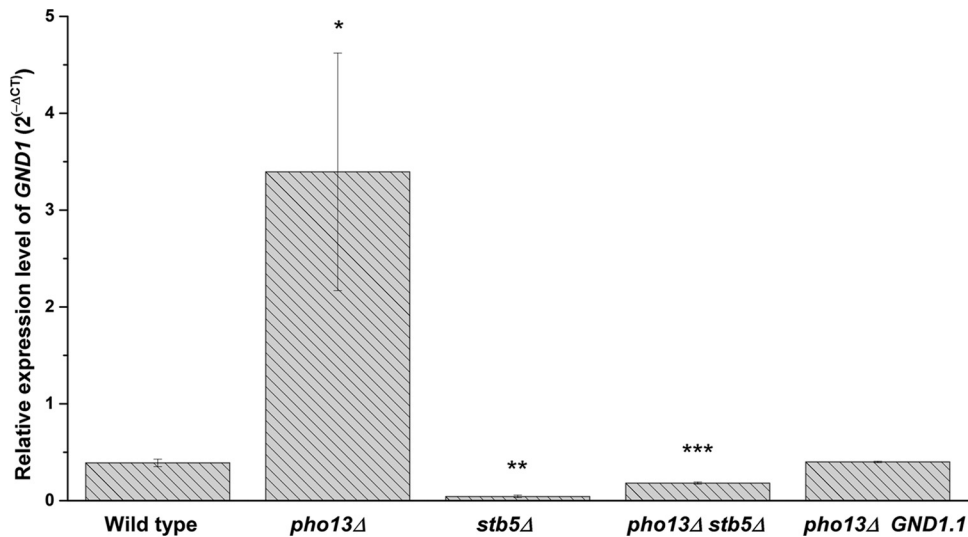


FIG 5 Fold change in the expression of transcription factors induced by *pho13Δ* during growth on different carbon sources ( $P < 0.05$ ).



**FIG 6** Upregulation of *GND1* by *pho13Δ* requires the transcription factor Stb5 and the Stb5-binding site of *GND1*. RT-qPCR was used to measure the expression of *GND1* in strains with *pho13Δ* or *stb5Δ*. The *pho13Δ GND1.1* mutant had an SNP (CTGTGTTA, where the SNP is underlined) in the Stb5-binding sequence (CGGTGTTA) upstream of the *GND1* coding region.

*stb5Δ* mutant, the level of *GND1* was only 10% of that in the wild-type strain, which supported the conclusion that the Stb5 transcription factor is required for PP pathway activation. Deletion of *PHO13* in the *stb5Δ* mutant (resulting in a *pho13Δ stb5Δ* mutant) did not upregulate *GND1*. These results suggest that Stb5 is necessary for the transcriptional upregulation induced by *pho13Δ*.

To confirm that Stb5 was responsible for the transcriptional changes induced by *pho13Δ*, we created a mutant in which Stb5 could not mediate the transcriptional regulation of *GND1*. A mutation was introduced in the Stb5-binding sequence (CGGTGTTA), located 262 bp upstream from the *GND1* coding region. Chromatin immunoprecipitation with microarray technology analysis has demonstrated that DNA oligonucleotides with an SNP in the binding sequence, such as CTGTGTTA (where the SNP is underlined), do not exhibit any detectable binding to Stb5 (22). Using a CRISPR-Cas system (20), we introduced an SNP (CTGTGTTA, where the SNP is underlined) into the Stb5-binding sequence of *GND1* *in vivo*, to generate *GND1.1*. When *GND1.1* was introduced into the *pho13Δ* strain, *GND1* upregulation was not detected, and the expression was the same as that in the wild-type strain (Fig. 6). The result strongly supports the conclusion that Stb5 mediates the transcriptional changes induced in the *pho13Δ* mutant.

**STB5 overexpression did not lead to the transcriptional activation of the *pho13Δ*-response genes.** Because the *pho13Δ* mutation resulted in the upregulation of *STB5*, we tested if the overexpression of *STB5* alone could activate the *pho13Δ*-response genes, such as *GND1*. When the *STB5* gene was overexpressed under the control of the strong and constitutive *TEF1* promoter, the mutant had a lower level of expression of *GND1* than the control strain (Fig. 7a). Moreover, the *STB5*-overexpressing mutant was not able to grow on xylose under a condition where the SR7 strain grew significantly (Fig. 7b). These results suggest that the upregulation of *STB5* is not sufficient to explain transcriptional changes induced by *pho13Δ*.

## DISCUSSION

The Pho13 enzyme in *S. cerevisiae* has received little attention because it is not directly related to any of the metabolic pathways in native strains and because its deletion does not produce a significant phenotype under standard culture conditions with glucose. On the other hand, three independent studies have found that *pho13Δ* improves xylose metabolism in strains engineered with a heterologous xylose-consuming pathway (11–13). Although the phenotypic improvement was significant, the mechanism was difficult to explain because xylose metabolism itself is not clearly understood in the engineered strains. Nevertheless, one study proposed that the xylulose-5-phosphate phosphatase activity of Pho13 might create a futile cycle when coupled with strong xylulokinase activity (12). Xylulokinase is a key enzyme connecting the heterologous xylose-consuming pathway to the native PP pathway (17).

However, the results of the present study suggest that Pho13 has other biochemical properties that are not dependent on xylose or the presence of the xylose pathway. Moreover, a previous study found that Pho13 had protein phosphatase activity against phosphoserine proteins (24), suggesting that Pho13 might be involved in protein signaling. Meanwhile, a spontaneous mutation in Pho13 improved the protein's specificity; the mutant form of Pho13 (G208D) was able to dephosphorylate a toxic intermediate in the purine biosynthesis pathway, 5-amino-4-imidazole *N*-succinocarboxamide ribonucleotide-5-phosphate (SAICAR), to generate the nontoxic riboside (25).

One hypothesis regarding the function of Pho13 is that *S. cerevisiae* Pho13 has a broad range of substrates and little specificity for the detoxification of sugar phosphates that accumulate to high levels. When 23 HAD-like phosphatases from *E. coli* were tested against 80 phosphorylated substrates, most enzymes exhibited substrate promiscuity with very wide and overlapping substrate ranges (26). Specifically, *E. coli* NagD, an *S. cerevisiae* Pho13 ortholog, had high specificities for both nu-

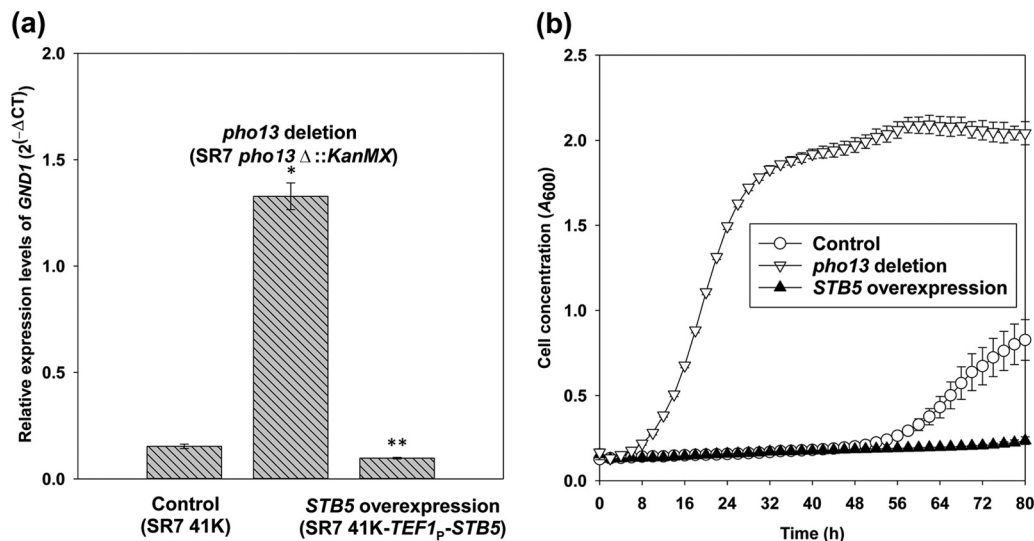


**FIG 7** A strain overexpressing *STB5* did not upregulate *GND1* (a) and did not grow on xylose (b). RT-qPCR was used to measure the expression of *GND1* in the control strain (SR7 41K), the *pho13* deletion mutant (SR7 *pho13* $\Delta$ ), and the *STB5*-overexpressing mutant (SR7 41K-*TEF1<sub>P</sub>*-*STB5*). The cell growth of the three strains was measured in YP medium containing 40 g/liter xylose for 80 h using a Bioscreen C plate reader system.

cleotide monophosphates (UMP and GMP) and sugar phosphates (ribose-5-phosphate and glucose-1-phosphate) (10, 26). Although NagD is expressed from the *N*-acetylglucosamine (GlcNAc) metabolic operon, it has no effect on metabolism (27). Because nonspecific HAD enzymes have broad and low substrate specificities and do not participate in specific metabolic pathways, it was previously proposed that nonspecific HAD enzymes detoxify sugar phosphates that accidentally accumulate at metabolic bottlenecks (9).

On the other hand, some eukaryotic orthologs of *S. cerevisiae* Pho13 have unique biological functions and specific substrates. Phosphoglycolate phosphatase 1 (Pgp1), a Pho13 ortholog in the plant *Arabidopsis thaliana*, contributes to the photorespiration pathway in chloroplasts (28). When the gene coding for Pgp1 was disrupted, the mutant was unable to grow in normal air (28). Interestingly, disruption of a cytosolic homolog of Pgp1, Pgp2, produced no phenotype, despite the fact that both enzymes have the same biochemical properties (28). Meanwhile, an *S. cerevisiae* Pho13 ortholog in humans was found to have pyridoxal phosphatase activity in the vitamin B<sub>6</sub> metabolic pathways (29).

Currently, it is not clear whether *S. cerevisiae* Pho13 is closely related to any bacterial or eukaryotic orthologs. However, other yeast orthologs, which have not been characterized, could provide more information about the enzymes in this subfamily. Specifically, investigation of native xylose-fermenting yeast, such as *S. stipitis* and *Neurospora crassa*, might be a good strategy for determining if the *pho13* $\Delta$ -induced signaling mechanism is conserved in yeast.

In this study, we identified a global transcriptional response induced by deletion of *PHO13* (*pho13* $\Delta$ ). In the *pho13* $\Delta$  mutant, an oxidative stress response was constitutively activated via the transcription factor Stb5. The stress response involved upregulation of PP pathway and NADPH-producing genes. The connection between Pho13 and Stb5 might be important for understanding the biological function of *S. cerevisiae* Pho13. Given that Stb5 is activated under NADPH-limiting conditions (22, 23), Pho13 could also be involved in cellular redox maintenance.

## ACKNOWLEDGMENTS

This work was supported by funding from the Energy Biosciences Institute to Soo Rin Kim and Yong-Su Jin.

## REFERENCES

- Ljungdahl PO, Daignan-Fornier B. 2012. Regulation of amino acid, nucleotide, and phosphate metabolism in *Saccharomyces cerevisiae*. *Genetics* 190:885–929. <http://dx.doi.org/10.1534/genetics.111.133306>.
- Saldanha AJ, Brauer MJ, Botstein D. 2004. Nutritional homeostasis in batch and steady-state culture of yeast. *Mol Biol Cell* 15:4089–4104. <http://dx.doi.org/10.1091/mbc.E04-04-0306>.
- van Heerden JH, Wortel MT, Bruggeman FJ, Heijnen JJ, Bollen YJM, Planqué R, Hulshof J, O'Toole TG, Wahl SA, Teusink B. 2014. Lost in transition: start-up of glycolysis yields subpopulations of nongrowing cells. *Science* 343:1245114. <http://dx.doi.org/10.1126/science.1245114>.
- Hunter T. 1995. Protein kinases and phosphatases: the yin and yang of protein phosphorylation and signaling. *Cell* 80:225–236. [http://dx.doi.org/10.1016/0092-8674\(95\)90405-0](http://dx.doi.org/10.1016/0092-8674(95)90405-0).
- Akiva E, Brown S, Almonacid DE, Barber AE, Custer AF, Hicks MA, Huang CC, Lauck F, Mashiyama ST, Meng EC, Mischel D, Morris JH, Ojha S, Schnoes AM, Stryke D, Yunes JM, Ferrin TE, Holliday GL, Babbitt PC. 2014. The structure-function linkage database. *Nucleic Acids Res* 42:D521–D530. <http://dx.doi.org/10.1093/nar/gkt1130>.
- Motosugi K, Esaki N, Soda K. 1982. Purification and properties of a new enzyme, DL-2-haloacid dehalogenase, from *Pseudomonas* sp. *J Bacteriol* 150:522–527.
- Lahiri SD, Zhang G, Dai J, Dunaway-Mariano D, Allen KN. 2004. Analysis of the substrate specificity loop of the HAD superfamily cap domain. *Biochemistry* 43:2812–2820. <http://dx.doi.org/10.1021/bi0356810>.
- Koonin EV, Tatusov RL. 1994. Computer analysis of bacterial haloacid dehalogenases defines a large superfamily of hydrolases with diverse specificity: application of an iterative approach to database search. *J Mol Biol* 244:125–132. <http://dx.doi.org/10.1006/jmbi.1994.1711>.
- Godinher LM, de Sá-Nogueira I. 2011. Characterization and regulation of a bacterial sugar phosphatase of the haloalkanoate dehalogenase superfamily, AraL, from *Bacillus subtilis*. *FEBS J* 278:2511–2524. <http://dx.doi.org/10.1111/j.1742-4658.2011.08177.x>.
- Tremblay LW, Dunaway-Mariano D, Allen KN. 2006. Structure and activity analyses of *Escherichia coli* K-12 NagD provide insight into the evolution of biochemical function in the haloalkanoic acid dehalogenase superfamily. *Biochemistry* 45:1183–1193. <http://dx.doi.org/10.1021/bi051842j>.
- Ni H, Laplaza JM, Jeffries TW. 2007. Transposon mutagenesis to improve the growth of recombinant *Saccharomyces cerevisiae* on D-xylose.



- Appl Environ Microbiol 73:2061–2066. <http://dx.doi.org/10.1128/AEM.02564-06>.
12. Kim SR, Skerker JM, Kang W, Lesmana A, Wei N, Arkin AP, Jin Y-S. 2013. Rational and evolutionary engineering approaches uncover a small set of genetic changes efficient for rapid xylose fermentation in *Saccharomyces cerevisiae*. PLoS One 8:e57048. <http://dx.doi.org/10.1371/journal.pone.0057048>.
  13. Fujitomi K, Sanda T, Hasunuma T, Kondo A. 2012. Deletion of the *PHO13* gene in *Saccharomyces cerevisiae* improves ethanol production from lignocellulosic hydrolysate in the presence of acetic and formic acids, and furfural. Bioresour Technol 111:161–166. <http://dx.doi.org/10.1016/j.biortech.2012.01.161>.
  14. Van Vleet JH, Jeffries TW, Olsson L. 2008. Deleting the paratrophyl phosphatase (pNPPase), *PHO13*, in recombinant *Saccharomyces cerevisiae* improves growth and ethanol production on D-xylose. Metab Eng 10:360–369. <http://dx.doi.org/10.1016/j.ymben.2007.12.002>.
  15. Li Y-C, Gou Z-X, Liu Z-S, Tang Y-Q, Akamatsu T, Kida K. 2014. Synergistic effects of *TAL1* over-expression and *PHO13* deletion on the weak acid inhibition of xylose fermentation by industrial *Saccharomyces cerevisiae* strain. Biotechnol Lett 36:2011–2021. <http://dx.doi.org/10.1007/s10529-014-1581-7>.
  16. Lee S-M, Jellison T, Alper H. 2014. Systematic and evolutionary engineering of a xylose isomerase-based pathway in *Saccharomyces cerevisiae* for efficient conversion yields. Biotechnol Biofuels 7:122. <http://dx.doi.org/10.1186/s13068-014-0122-x>.
  17. Kim SR, Park Y-C, Jin Y-S, Seo J-H. 2013. Strain engineering of *Saccharomyces cerevisiae* for enhanced xylose metabolism. Biotechnol Adv 31: 851–861. <http://dx.doi.org/10.1016/j.biotechadv.2013.03.004>.
  18. Hegemann J, Heick S. 2011. Delete and repeat: a comprehensive toolkit for sequential gene knockout in the budding yeast *Saccharomyces cerevisiae*, p 189–206. In Williams JA (ed), Strain engineering, vol 765. Humana Press, Totowa, NJ.
  19. Gietz RD, Schiestl RH. 2007. High-efficiency yeast transformation using the LiAc/SS carrier DNA/PEG method. Nat Protoc 2:31–34. <http://dx.doi.org/10.1038/nprot.2007.13>.
  20. DiCarlo JE, Norville JE, Mali P, Rios X, Aach J, Church GM. 2013. Genome engineering in *Saccharomyces cerevisiae* using CRISPR-Cas systems. Nucleic Acids Res 41:4336–4343. <http://dx.doi.org/10.1093/nar/gkt135>.
  21. Livak KJ, Schmittgen TD. 2001. Analysis of relative gene expression data using real-time quantitative PCR and the  $2^{-\Delta\Delta CT}$  method. Methods 25: 402–408. <http://dx.doi.org/10.1006/meth.2001.1262>.
  22. Laroche M, Drouin S, Robert F, Turcotte B. 2006. Oxidative stress-activated zinc cluster protein Stb5 has dual activator/repressor functions required for pentose phosphate pathway regulation and NADPH production. Mol Cell Biol 26:6690–6701. <http://dx.doi.org/10.1128/MCB.02450-05>.
  23. Hector RE, Bowman MJ, Skory CD, Cotta MA. 2009. The *Saccharomyces cerevisiae* *YMR315W* gene encodes an NADP(H)-specific oxidoreductase regulated by the transcription factor Stb5p in response to NADPH limitation. New Biotechnol 26:171–180. <http://dx.doi.org/10.1016/j.nbt.2009.08.008>.
  24. Tuleva B, Vasileva-Tonkova E, Galabova D. 1998. A specific alkaline phosphatase from *Saccharomyces cerevisiae* with protein phosphatase activity. FEMS Microbiol Lett 161:139–144. <http://dx.doi.org/10.1111/j.1574-6968.1998.tb12940.x>.
  25. Hürlimann HC, Laloo B, Simon-Kayser B, Saint-Marc C, Coudrier F, Lemoine S, Daignan-Fornier B, Pinson B. 2011. Physiological and toxic effects of purine intermediate 5-amino-4-imidazolecarboxamide ribonucleotide (AICAR) in yeast. J Biol Chem 286:30994–31002. <http://dx.doi.org/10.1074/jbc.M111.262659>.
  26. Kuznetsova E, Proudfoot M, Gonzalez CF, Brown G, Omelchenko MV, Borozan I, Carmel L, Wolf YI, Mori H, Savchenko AV, Arrowsmith CH, Koonin EV, Edwards AM, Yakunin AF. 2006. Genome-wide analysis of substrate specificities of the *Escherichia coli* haloacid dehalogenase-like phosphatase family. J Biol Chem 281:36149–36161. <http://dx.doi.org/10.1074/jbc.M605449200>.
  27. Peri KG, Goldie H, Waygood EB. 1990. Cloning and characterization of the N-acetylglucosamine operon of *Escherichia coli*. Biochem Cell Biol 68:123–137. <http://dx.doi.org/10.1139/o90-017>.
  28. Schwarte S, Bauwe H. 2007. Identification of the photorespiratory 2-phosphoglycolate phosphatase, PGLP1, in Arabidopsis. Plant Physiol 144:1580–1586. <http://dx.doi.org/10.1104/pp.107.099192>.
  29. Jang YM, Kim DW, Kang T-C, Won MH, Baek N-I, Moon BJ, Choi SY, Kwon O-S. 2003. Human pyridoxal phosphatase: molecular cloning, functional expression, and tissue distribution. J Biol Chem 278:50040–50046. <http://dx.doi.org/10.1074/jbc.M309619200>.
  30. Güldener U, Heck S, Fiedler T, Beinhauer J, Hegemann JH. 1996. A new efficient gene disruption cassette for repeated use in budding yeast. Nucleic Acids Res 24:2519–2524. <http://dx.doi.org/10.1093/nar/24.13.2519>.
  31. Baker Brachmann C, Davies A, Cost GJ, Caputo E, Li J, Hieter P, Boeke JD. 1998. Designer deletion strains derived from *Saccharomyces cerevisiae* S288C: a useful set of strains and plasmids for PCR-mediated gene disruption and other applications. Yeast 14:115–132. [http://dx.doi.org/10.1002/\(SICI\)1097-0061\(19980130\)14:2<115::AID-YEA204>3.0.CO;2-2](http://dx.doi.org/10.1002/(SICI)1097-0061(19980130)14:2<115::AID-YEA204>3.0.CO;2-2).
  32. Gievers G, Chu AM, Ni L, Connelly C, Riles L, Veronneau S, Dow S, Lucau-Danila A, Anderson K, Andre B, Arkin AP, Astromoff A, El Bakkoury M, Bangham R, Benito R, Brachat S, Campanaro S, Curtiss M, Davis K, Deutschbauer A, Entian K-D, Flaherty P, Foury F, Garfinkel DJ, Gerstein M, Gotte D, Güldener U, Hegemann JH, Hempel S, Herman Z, Jaramillo DF, Kelly DE, Kelly SL, Kotter P, LaBonte D, Lamb DC, Lan N, Liang H, Liao H, Liu L, Luo C, Lussier M, Mao R, Menard P, Ooi SL, Revuelta JL, Roberts CJ, Rose M, Ross-Macdonald P, Scherens B, et al. 2002. Functional profiling of the *Saccharomyces cerevisiae* genome. Nature 418:387–391. <http://dx.doi.org/10.1038/nature00935>.
  33. Hosaka K, Nikawa J-i, Kodaki T, Yamashita S. 1992. A dominant mutation that alters the regulation of *INO1* expression in *Saccharomyces cerevisiae*. J Biochem 111:352–358.